03

Influence of turbulent flow formation conditions on coherent structures and velocity pulsations

© D.Yu. Zhilenko, O.E. Krivonosova

Institute of Mechanics of Lomonosov Moscow State University, Moscow, Russia
E-mail: jilenko@imec.msu.ru

Received September 18, 2024
Revised November 7, 2024
Accepted November 7, 2024

Turbulent flows of viscous incompressible fluid in a spherical layer are numerically investigated. Two ways of flow formation are considered: sequential and simultaneous increase of the counter-rotation velocity of spherical boundaries from the resting state. It is found that at equal Reynolds numbers, but different ways of flow formation, types of spatial coherent structures, levels of velocity pulsations and their spectra differ.

Keywords: non-uniqueness of turbulent flows, spherical Couette flow.

DOI: 10.61011/TPL.2025.03.60717.20124

Large-scale coherent structures [1–5] can be observed in flows near the threshold of turbulence formation. Such structures may result from linear instability of both laminar flows preceding the onset of turbulence [1,5] and turbulent flows [6,7]. The existence of coherent structures is assumed to be supported by fluctuations in turbulence energy [1], but the problem of the interaction between structures and chaotic components has not yet been solved [4]. This paper addresses turbulence in spherical Couette flow (SCF) — the flow of a viscous incompressible fluid due to the rotation of coaxially arranged spheres. The interest in turbulence in rotating flows is due to the need to suppress [8] it, for example, in liquid metal and melt [9] processing technologies. As found in [10,11], the possibilities of turbulence formation in SCF and its properties are determined by the prehistory of flow development. In [11], under the condition of equal Reynolds numbers for the inner and outer spherical boundaries, it is experimentally shown that the properties of turbulent flows (type of spectrum and values of correlation dimensionality) differ in different ways of their formation. In other cases, the issue of the dependence of the properties of three-dimensional turbulent flows of viscous incompressible fluid on their prehistory is still open, which determines the purpose of this paper.

The flow of a viscous incompressible fluid is described by the equations of Navier –Stokes and continuity

$$\frac{\partial \mathbf{U}}{\partial t} = \mathbf{U} \times \operatorname{rot} \mathbf{U} - \operatorname{grad}\left(\frac{p}{\rho} + \frac{\mathbf{U}^2}{2}\right) - \nu \operatorname{rot}\operatorname{rot} \mathbf{U}, \quad \operatorname{div} \mathbf{U} = 0$$

with the conditions of no-slip and impermeability at the boundaries in the spherical coordinate system:

$$u_\varphi(r = r_k) = \Omega_k(t) r_k \sin\theta, \quad u_r(r = r_k) = 0,$$

$$u_\theta(r = r_k) = 0, \quad k = 1, 2.$$

Here $\mathbf{U}$ — velocity field, p — pressure, ρ — density, ν — kinematic viscosity of the fluid in the layer, u_φ, u_r, u_θ — the azimuthal, radial, and polar velocity components, respectively, Ω_1 and Ω_2 — rotational angular velocities, and r_1 and r_2 — the radii of the inner and outer spheres, respectively (index 1 refers to the inner sphere, 2 — to the outer sphere).

The numerical solution method is based on a conservative finite-difference scheme for discretizing the Navier–Stokes equations over space and a semi-implicit Runge–Kutta scheme of third-order accuracy for time integration, the algorithm is investigated in detail in [12], and in the special case of a three-dimensional problem in a spherical coordinate system using nonuniform θ and r grids — in [13]. The full system of equations was solved with discretization over space on non-uniform on r and θ grids with a total number of nodes $5.76 \cdot 10^5$ and a ratio of maximum cell size to minimum cell size 4. The convergence of the computational results as the number of nodes increases is studied in detail in [13–15]. The calculations were performed using the parameters corresponding to those of the experiment [11]: $\nu = 5 \cdot 10^{-5}\,\mathrm{m^2/s}$, $r_2 = 0.15\,\mathrm{m}$, $r_1 = 0.075\,\mathrm{m}$ (relative layer thickness $\sigma = (r_2 - r_1)/r_1 = 1$). We consider two ways of forming turbulent flows at $\mathrm{Re}_2 = \Omega_2 r_2^2/\nu = -900$ (the minus sign in front of one of the Reynolds numbers is used to denote the opposite direction of boundary rotation). The first method, let us call it asynchronous, starts with $\mathrm{Re}_1 = \Omega_1 r_1^2/\nu = 0$. Then Re_1 is varied at a constant Re_2. In the second method, let's call it synchronous, the angular velocities of rotation of both boundaries are simultaneously varied from the state of rest to selected values of Re_1. The values Re_1 were chosen near the threshold of the transition to turbulence $\mathrm{Re}_{1t} = 450$ [14]: $\mathrm{Re}_1 = 460$, 470 and 490. The time step is constant $\Delta t = 1.2 \cdot 10^{-2}\,\mathrm{s}$, which provided 120–128 steps per rotation of the inner sphere. The duration of each calculation variation was 5400 s, and the averaged values were calculated over the last 2100 s.

Just as in [14], the azimuthal velocity distribution u_φ in θ–φplane is considered as coherent structures. In

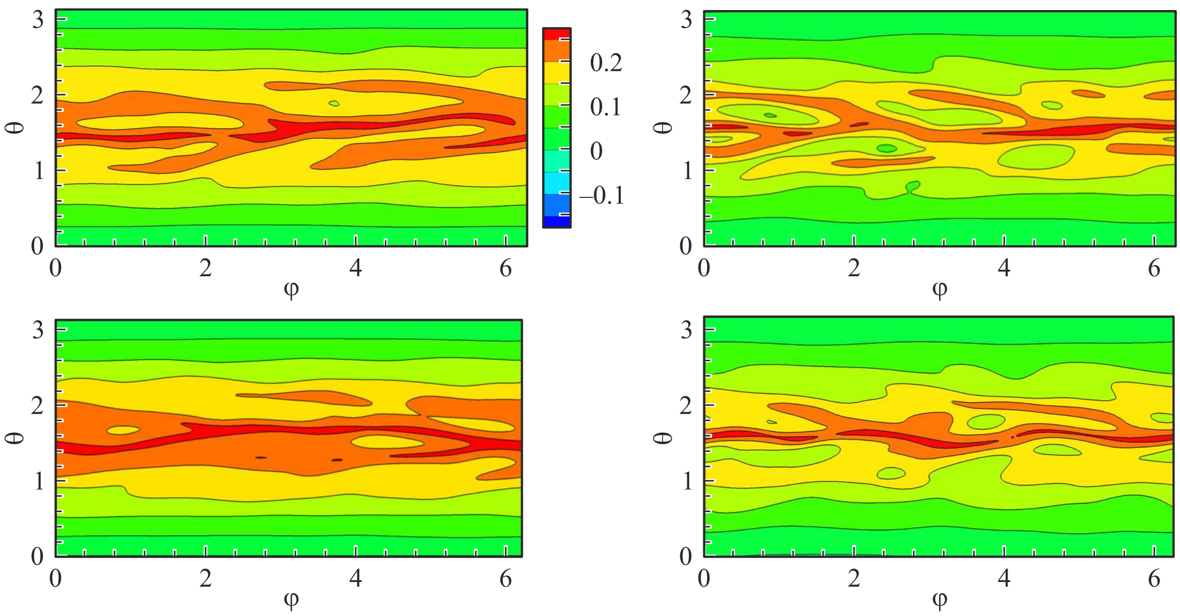

Figure 1. The azimuthal velocity distribution u_φ [m/s] in the $\theta-\varphi$ plane at a distance 0.07σ from the inner sphere. From the top — asynchronous way of forming flows, from the bottom — synchronous. From left — $\mathrm{Re}_1 = 460$, from right— $\mathrm{Re}_1 = 490$. A color version of the figures is presented in the online version of the paper.

the asynchronous way of turbulence formation in [14] it is shown that at$\mathrm{Re}_1 = 450$ and $\mathrm{Re}_2 = -900$ a coherent structure in the form of an azimuthal wave with wave number$m = 3$ ([14], Fig. 1, b) can be identified at a distance of 0.2σ from the internal sphere. In this paper, it was found that, regardless of the turbulence formation method, the same coherent structures dominate in the region between the outer sp here and the circulation interface defined by the $u_\varphi = 0$condition. Near the inner sphere not only the type of coherent structures changes with various methods of turbulence formation, but also the degree of their coherence, understood as the possibility of distinguishing the dominant wave number in the azimuthal direction. Thus, at $\mathrm{Re}_1 = 460$ (left part of Fig. 1), the wave number $m = 2$is observed on the upper fragment (asynchronous method), whereas there is no dominant number m on the lower fragment (synchronous method). The opposite is true in the right part of Fig. 1 for $\mathrm{Re}_1 = 490$: at the top (asynchronous method), a combination of $m = 2$ and $m = 3$ is observed (this structure is not kept constant because waves with $m = 2$ and $m = 3$ propagate with different phase velocities [13,15]), while at the bottom (synchronous method) the dominant is $m = 3$. Thus, in the case of $\mathrm{Re}_1 = 460$ the degree of coherence of spatial structures is higher in the asynchronous method, and in the case of $\mathrm{Re}_1 = 490$ — in the synchronous method of flow formation. Let us further consider the amplitudes of fluctuations of the azimuthal component of the kinetic energy of $E_\varphi-\mathrm{rms}\,E_\varphi$ flows

$$E_\varphi = \int u_\varphi^2(r,\theta,t), \;\; \mathrm{rms}\,E_\varphi = \sqrt{\frac{1}{I-1}\sum_{i=1}^{I}\left(E_\varphi(t_i) - E_{\varphi_0}\right)^2}.$$

Table 1. Normalized values of the standard deviations of the azimuthal component of the kinetic energy of the flows' kinetic energy

Re_1	$\left((\mathrm{rms}\,E_\varphi)/E_\varphi\right)_A$ asynchronous method	$\left((\mathrm{rms}\,E_\varphi)/E_\varphi\right)_S$ synchronous method
460	0.00556	0.00576
470	0.00606	0.00613
490	0.00714	0.00664

Value $E_\varphi$is determined by integrating the azimuthal component of the flow velocity over the entire volume of the spherical layer $E_\varphi(t)$ andE_{φ_0} — the instantaneous and average values of the azimuthal component of the flow kinetic energy, respectively. It can be seen from Table 1 that at $\mathrm{Re}_1 = 460$ rms E_φ is smaller for the asynchronous method, and at $\mathrm{Re}_1 = 490$ — smaller for the synchronous method. Comparison of Fig. 1 and Table 1 indicates a correlation between the degree of spatial structure coherence and the magnitudes of fluctuations E_φ: the higher the degree of coherence, the lower the amplitude of fluctuations E_φ,which is consistent with the available ideas about the interaction between coherent structures and velocity fluctuations [1]. Figure 2 shows the distribution of the ratio of the amplitude ratio of the velocity fluctuations of the flows $R = \mathrm{rms}(u_\varphi)_S/\mathrm{rms}(u_\varphi)_A$ from the dimensionless distance $\delta = (r-r_1)/(r_2-r_1)$, where index S refers to the synchronous method, A — to asynchronous one. Value R at all latitudes and at all values of Re_1 has local extrema. The highest and lowest values of R

Table 2. Local regions of flows, in which the type of velocity pulsation spectra changes under different methods of flow formation (2D — spectra corresponding to two-dimensional turbulence, 3D — spectra corresponding to three-dimensional turbulence).

Re_1	θ	δ	View of the spectrum		R (from Fig. 2)
			Synchronous method	Asynchronous method	
460	21.3	0.135	3D	2D	> 1
460	52.9	0.61, 0.7	2D	3D	< 1
470	21.3	0.134, 0.25, 0.36	2D	3D	< 1
470	52.9	0.7, 0.8	2D	3D	< 1
470	89.8	0.8	2D	3D	< 1
470	89.8	0.25	3D	2D	> 1
490	21.3	0.8	2D	3D	< 1
490	89.8	0.25	2D	3D	< 1

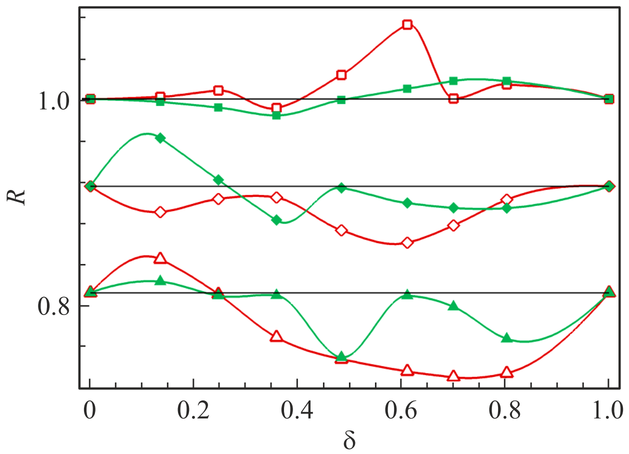

Figure 2. Dependence of the value of R onδ. Squares — $\theta = 89.8^\circ$ (equatorial plane), diamonds — $\theta = 52.9^\circ$ (middle latitudes), triangles — $\theta = 21.3^\circ$ (circumpolar region). Red (uncolored symbols) — Re_1=460, green (colored symbols) — Re_1=490. For clarity, the curves at different values of θ are shifted on the ordinate axis, with horizontal black lines corresponding to $R = 1$.

are observed at $Re_1 = 460$ in the equatorial plane and in the circumpolar region, respectively. At different methods of flow formation, velocity fluctuations differ not only in intensity but also in the type of spectra (Fig. 3). In the synchronous method, the spectra characteristic of two-dimensional turbulence (2D) with a reverse energy transfer cascade (dependence of the energy spectrum $E(k)$ on wave number k in the form$E(k) \sim k^{-3}$), are observed at mid-latitudes ($Re_1 = 460$, 470), near the rotation axis, and in a part of the equatorial plane ($Re_1 = 470$, 490). With the asynchronous method, spectra characteristic of three-dimensional turbulence (3D) with a direct energy transfer cascade ($E(k) \sim k^{-5/3}$ and $E(k) \sim k^{-11/5}$) are obtained in the same flow regions. It is well known [16] that regions with different types of spectra can be formed in flows with rotation. Table 2 shows the coordinates of the points where different types of spectra were obtained by different formation methods. Comparison of Table 2 and Figure 2 shows that these points lie in the regions of local extrema of the $R(\delta)$ dependence, i.e., in the regions of change in the fluctuation intensity of flow velocity. The last column of Table 2 shows the values of R at the corresponding points. It can be seen that at the same Re_1 local maxima of azimuthal velocity fluctuations correspond to three-dimensional turbulence, and local minima — to two-dimensional one.

The obtained results show a general relationship between all the properties of turbulence discussed above: the higher the coherence degree of large-scale spatial structures, the lower the intensity of kinetic energy pulsations. In its turn, the maximum decrease in the intensity of velocity pulsations in local flow regions leads to two-dimensional turbulence with energy transfer from smaller scales to larger ones, where coherent structures are observed. On the contrary, as the coherence degree of spatial structures decreases, kinetic energy pulsations increase, as well as

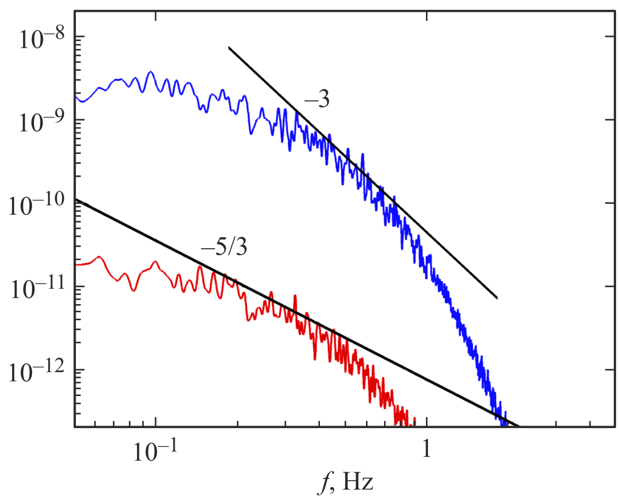

Figure 3. Azimuthal velocity pulsation spectra at $Re_1 = 490$, $\theta = 21.3^\circ$ at distance 0.8σ from the inner sphere. Red (lower curve) shows asynchronous method, blue (upper curve) — synchronous method, straight lines — approximation of the spectra slopes.

velocity fluctuations, and three-dimensional turbulence is observed. The processes of energy exchange between velocity fluctuations and the main flow are currently being extensively studied [17].

Funding

The research was supported by a grant from the Russian Science Foundation (project № 23-29-00051).

Conflict of interest

The authors declare that they have no conflict of interest.

References

[1] J. Jimenez, J. Fluid Mech., **842**, 1 (2018). DOI: 10.1017/jfm.2018.144
[2] S.T. Salesky, W. Anderson, Phys. Rev. Lett., **125**, 124501 (2020). DOI: 10.1103/PhysRevLett.125.124501
[3] M.D. Graham, D. Floryan, Annu. Rev. Fluid Mech., **53**, 227 (2021). DOI: 10.1146/annurev-fluid-051820-020223
[4] D.S. Agafontsev, E.A. Kuznetsov, A.A. Mailybaev, E.V. Sereshchenko, UVN, **192** (2), 205 (2022). (in Russian). DOI: 10.3367/ UFNr.2020.11.038875 [D.S. Agafontsev, E.A. Kuznetsov, E.V. Sereshenko, A.A. Mailybaev, Phys. Usp., **65** (2), 189 (2022). DOI: 10.3367/ufne.2020.11.038875].
[5] A. Guseva, S.M. Tobias, Phil. Trans. R. Soc. A, **381**, 20220120 (2023). DOI: 10.1098/rsta.2022.0120
[6] P.V. Kashyap, Y. Duguet, O. Dauchot, Phys. Rev. Lett., **129**, 244501 (2022). DOI: 10.1103/PhysRevLett.129.244501
[7] J. Page, P. Norgaard, M.P. Brenner, R.R. Kerswell, PNAS, **121** (23), e2320007121 (2024). DOI: 10.1073/pnas.2320007121
[8] D.Yu. Zhilenko, O.E. Krivonosova, Tech. Phys. Lett., **45** (9), 870 (2019). DOI: 10.1134/S1063785019090141.
[9] A.I. Prostomolotov, N.A. Verezub, *Mekhanika protsessov polucheniya kristallicheskikh materialov* (NITU „MISiS," M. 2023) (in Russian). DOI: 10.61726/5600.2024.15.25.001
[10] Yu.N. Belyaev, I.M. Yavorskaya, Fluid Dyn., **26** (1), 7 (1991). DOI: 10.1007/BF01050106.
[11] D.Yu. Zhilenko, O.E. Krivonosova, Fluid Dyn., **43** (5), 698 (2008). DOI: 10.1134/S0015462808050037.
[12] N. Nikitin, J. Comp. Phys., **217**, 759 (2006). DOI: 10.1016/j.jcp.2006.01.036).
[13] O.E. Krivonosova, *Perehod k stochastichnosti v shirokom spchericheskom sloe pri vstrechnom vraschenii granits: pryamoi rasschet i experiment* avtoreferat kand.dis. (MSU, M., 2007). (in Russian).
[14] D.Yu. Zhilenko, O.E. Krivonosova, Tech. Phys., **55** (4), 449 (2010). DOI: 10.1134/S1063784210040031.
[15] D.Yu. Zhilenko, O.E. Krivonosova, Tech. Phys. Lett., **39** (1), 84 (2013). DOI: 10.1134/S1063785013010276.
[16] K. Seshasayanan, B. Gallet, J. Fluid Mech., **901**, R5 (2020). DOI: 10.1017/jfm.2020.541
[17] B. Tripathi, P.W. Terry, A.E. Fraser, E.G. Zweibel, M.J. Pueschel, Phys. Fluids, **35**, 105151 (2023). DOI: 10.1063/5.0167092

Translated by J.Savelyeva